Improving Equation of State Tables

Priya Rajasethupathy

Advisor: Dr. Jacques Delettrez

University of Rochester

Laboratory for Laser Energetics

Summer High School Research Program 2000

Inertial Confinement Fusion is based on the idea of imploding a target (filled with deuterium and tritium gas) in an attempt to release energy in the form of neutrons. To understand and predict target behavior during the fusion process, it is necessary to produce accurate simulations of the implosion. The equation of state (EOS) forms an indispensable part of these simulations. In this project several available EOS, both tabular and analytic, were compared. Also, the concept of interpolation from tables as an alternative to using analytic expressions was considered and the accuracy of various interpolation methods was evaluated.

1. Introduction

Currently our Earth has three major sources of energy: fossil fuels, nuclear fission, and solar energy. However, all three sources have their share of disadvantages, whether it be in atmospheric pollution, inefficiency, or limited resources. Hence the question arises: "What source of energy is clean, safe, feasible, and inexhaustible?" As we step into the next millennium, the concept of Inertial Confinement Fusion (ICF) as a viable alternative to fossil fuels, is gaining interest and momentum. Looking at our sun

as a prime example of ICF, it becomes appealing for us to try and artificially create this naturally occurring phenomenon.

ICF is characterized by a series of fusion reactions between nuclei of light elements, releasing energy in the process. The Equation of State (EOS) performs a vital role in simulating this process as it is used to determine the pressure, heat capacity, and energy of a material under all conditions of temperature and density. Therefore, EOS is useful in not only understanding ICF, but also in predicting the end result.

As of now, there are four EOS tables that are available for computer simulations at LLE. They include SESAME tables[3] (from Los Alamos National Laboratory, NM), LEOS tables[2] (from Lawrence Livermore National Laboratory, CA), tabular Thomas-Fermi tables[4] (from Laboratory for Laser Energetics, NY), and Thomas-Fermi analytic tables[1] (from Rutherford Appleton Laboratory, UK). All four tables provide EOS for aluminum, plastic, and a 50/50 deuterium/tritium gas (all of which are present in most targets). One objective of this project was to compare the different tables, keeping in mind the fact that for cold and warm dense plasma (near solid densities and temperatures from 0.01 to 100 eV) equations of state are not well known. Another goal was to create a new equation of state table, from the analytic EOS, primarily to produce faster run-times on computers. This permitted us to study interpolation methods and their accuracy.

2. Comparison of EOS tables

Before discussing the similarities and differences between the EOS tables, it is helpful to introduce the units of measurement that are consistently used across all four tables mentioned in section 1. Temperature is measured in electron volts (1eV =11604K),

density is measured in grams per centimeter cubed (g/cm^3), pressure is measured in megabars (Mb), energy is measured in ergs per atom (ergs/atom), and finally heat capacity is measured in ergs per atom per degree Kelvin (ergs/atom/^oK). Temperatures of interest range from 2.5 x 10^{-2} eV (room temperature) to 32 keV, while the densities densities range from 1.e-3 to 1000 g/cm^3.

First, we compare the pressure of deuterium gas between SESAME and LEOS (Fig. 1). The relative agreement between two independent tables increases our confidence in the accuracy of these tables. Next, we compare the analytic and tabular Thomas-Fermi EOS for pressure, energy, and heat capacity, each as a function of temperature and density. Thomas-Fermi EOS needs a quantum mechanical correction to describe conditions for a warm dense plasma. A correction is applied only to the electron pressure in the tabular Thomas-Fermi and to all quantities in the analytic Thomas-Fermi EOS. As a result, while both tables agree fairly well in computing pressure (Fig. 2), they disagree to a large extent when calculating energy (Fig. 3) and heat capacity (Fig. 4). As expected all three variables show good agreement in the ideal gas region ($T > 1$ keV).

Since the analytic and tabular Thomas-Fermi EOS differ, we turn to SESAME and LEOS to resolve the disagreement, or at least distinguish the correct table from the incorrect. Comparing the analytic Thomas-Fermi EOS with SESAME confirms that the analytic code is more accurate than tabular Thomas-Fermi for pressure (Fig. 5) and energy (Fig. 6), but not for heat capacity (Fig. 7). Similar comparisons with respect to aluminum confirm the above conclusions as seen in Figs. 8, 9, and 10.

Thus, the conclusion obtained from comparing the EOS tables is that the analytic Thomas-Fermi EOS is more reliable than the tabular Thomas-Fermi EOS (except for heat

capacity). In addition to being more accurate, the analytic EOS is advantageous because it finds pressure or heat capacity for any specific values of temperature and density, whereas the tabular EOS needs to be interpolated.

3. Interpolation methods

The analytic EOS gives us the opportunity to test interpolation methods and to check whether interpolation from tables is faster than calculating analytic expressions. To that end, a table was created from the analytic EOS, which we call "tabulated analytic EOS".

When comparing interpolation methods with analytic computation, the two major factors involved are speed and accuracy. To find the values for pressure and energy, we decided to interpolate from the tabulated analytic EOS. However, to find the specific heat, we need to calculate the derivative of the interpolated energy value. The following methods were used to find interpolated values for the energy (e) and the specific heat (C_v) at point x with values T and d for temperature and density:

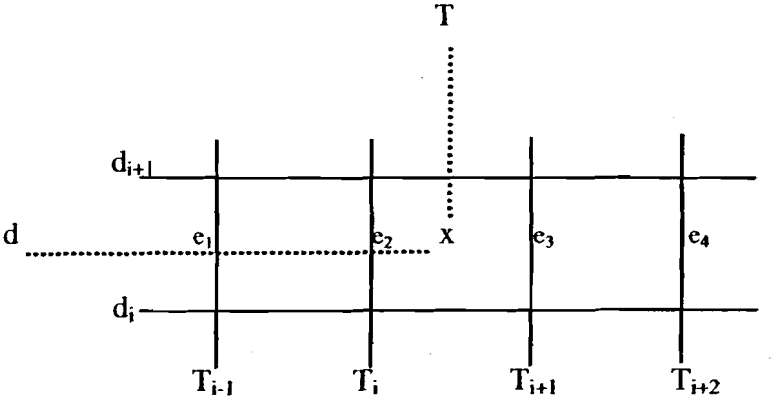

The energy was interpolated using two methods:

1. The first method calculates the derivative at $e(t_i,d_i)$, to approximate the behavior of the curve at point x.

$$e(T,d) = e(T_i,d_i) + \left(\frac{de}{dd_i}\right)_{T_i}(d-d_i) + \left(\frac{de}{dT_i}\right)_{d_i}(T-T_i)$$

$$e(T,d) = e(T_i,d_i) + \frac{e(T_i,d_{i+1}) - e(T_i,d_i)}{d_{i+1}-d_i}(d-d_i) + \frac{e(T_{i+1},d_i) - e(T_i,d_i)}{T_{i+1}-T_i}(T-T_i)$$

(1)

2. The second method interpolates bi-linearly (in two directions). Thus, first we interpolate along the temperature axis over the densities, and then along the density axis over the temperatures, to approximate the value of the curve at point x.

$$e_2 = e(T_i,d_i) + (d-d_i)\frac{e(T_i,d_{i+1}) - e(T_i,d_i)}{d_{i+1}-d_i}$$

$$e_3 = e(T_{i+1},d_i) + (d-d_i)\frac{e(T_{i+1},d_{i+1}) - e(T_{i+1},d_i)}{d_{i+1}-d_i}$$

$$e(T,d) = e_2 + (T-T_i)\frac{e_3-e_2}{T_{i+1}-T_i} \qquad (2)$$

The specific heat, which is the first derivative of energy with respect to temperature at constant volume, was interpolated using one method.

1. This method first calculates the 'centered' derivatives at the temperature grid points from the interpolated values e_1, e_2, e_3, and e_4 as defined when deriving Eq. 2.

$$e'_2 = \frac{e_3 - e_1}{T_{i+1} - T_{i-1}} \qquad e'_3 = \frac{e_4 - e_2}{T_{i+2} - T_i}.$$

Now the value at x can be found by linearly interpolating over the temperature.

$$C_v = \frac{d\{e(T,d)\}}{dT} = e'_2 + \left(\frac{e'_3 - e'_2}{T_{i+1} - T_i} \right)(T - T_i). \tag{3}$$

We considered evaluating spline interpolation for speed and accuracy, but it still remains to be done.

3.2 Accuracy and speed of interpolation methods versus analytic computation

When comparing the interpolation methods for energy with the analytic EOS code, the second method was more accurate (Fig. 11), showing less than 0.3 percent error. When comparing the interpolation methods for specific heat with the analytic EOS code (Fig. 12) results showed less than 1 percent error. Thus, the interpolation methods show good accuracy.

When computing the run-time, both interpolation methods ran at about the same speed, and were both more than 200 times faster than the analytic EOS code. When both codes were looped 1 million times, the interpolation code was completed in 0.12s while the analytic code took 28. 47s. Even with this enormous time difference, it is actually possible to widen this gap even further by traversing the table more efficiently (performing a binary search rather than a sequential search). Our conclusion is that the

speed of the interpolated EOS outweighs any slight inaccuracies in the methods and is a very efficient method of calculating EOS quantities.

3.2 Scaling of tabulated values before interpolation

The density and temperature grid points in the SESAME and LEOS tables are obtained by dividing $\log_{10}$ decades into equal spacing. The resulting grid points are then not equally spaced. We call these tables "logarithmically scaled" tables. The analytic EOS table was created with the same grid pattern. In an attempt to improve the accuracy of the interpolation, we created a "linearly scaled" analytic EOS table consisting of the $\log_{10}$ of all values. The resulting temperature and density grid points are then equally spaced. Certainly, it seems that a logarithmic curve would be harder to bi-linearly interpolate than a linear curve. However, when the two were compared, it was found that logarithmically (Fig. 12) interpolating was actually more accurate than linearly interpolating (Fig. 13):

$$\text{Logarithmic interpolation: } \frac{de}{dt} \text{ (same as Eq. 3)}$$

$$\text{Linear interpolation: } \frac{de}{dT} = \frac{d\ln e}{d\ln T}\left(\frac{e}{T}\right)$$

Linear interpolation is inaccurate because it involves not only calculating the derivative, but also multiplying by the energy value. This is the problem because the energy values can be several magnitudes apart between two temperature grid points. This becomes clearer when looking at figure 12, in which the specific heat (C_v) takes a big jump at a temperature of 1eV because the energy graph shows a very steep gradient at that

temperature. Thus we conclude that, for general interpolation linear scaling is appropriate, but when taking the derivative it is better to use logarithmic scaling.

4. Conclusion

This project produces three conclusions. Firstly, it was found that the Thomas-Fermi analytic EOS matched SESAME and LEOS tables more closely than tabular Thomas-Fermi EOS, which makes the analytic EOS more accurate and reliable. Secondly, we found that interpolating from tables is more than 200 times faster than analytic calculation. This led to the creation of another EOS table - the interpolated or tabulated analytic EOS. Finally, in general, linear scaling enables the tabulation of more accurate interpolated values. However, when interpolation requires computing derivatives, logarithmic interpolation is more accurate.

Acknowledgements

First and foremost, I would like to sincerely thank my advisor Dr. Jacques Delettrez for not only his time and advice, but also for his continued patience and support. My experience at LLE would not have been the same without him. I would like to give a special thanks to the many scientists in the lab, especially those in the theory division Drs. Radha, Epstein, and Town, who were both approachable and helpful. Finally, I would like to thank the other students of the program for truly making this experience a memorable one.

References

1. A.R.Bell, "*New Equations of State for Medusa*", Report FL-80-091, Rutherford Appleton laboratories (1980).
2. D.A.Young, (private communication, 2000)
3. J. Abdallah Jr. et al, HYDSES, "*A subroutine package for using SESAME in Hydrodynamic codes*", LANL report LA-8209 (1980)
4. S. Skupsky, (private communication, 1975)

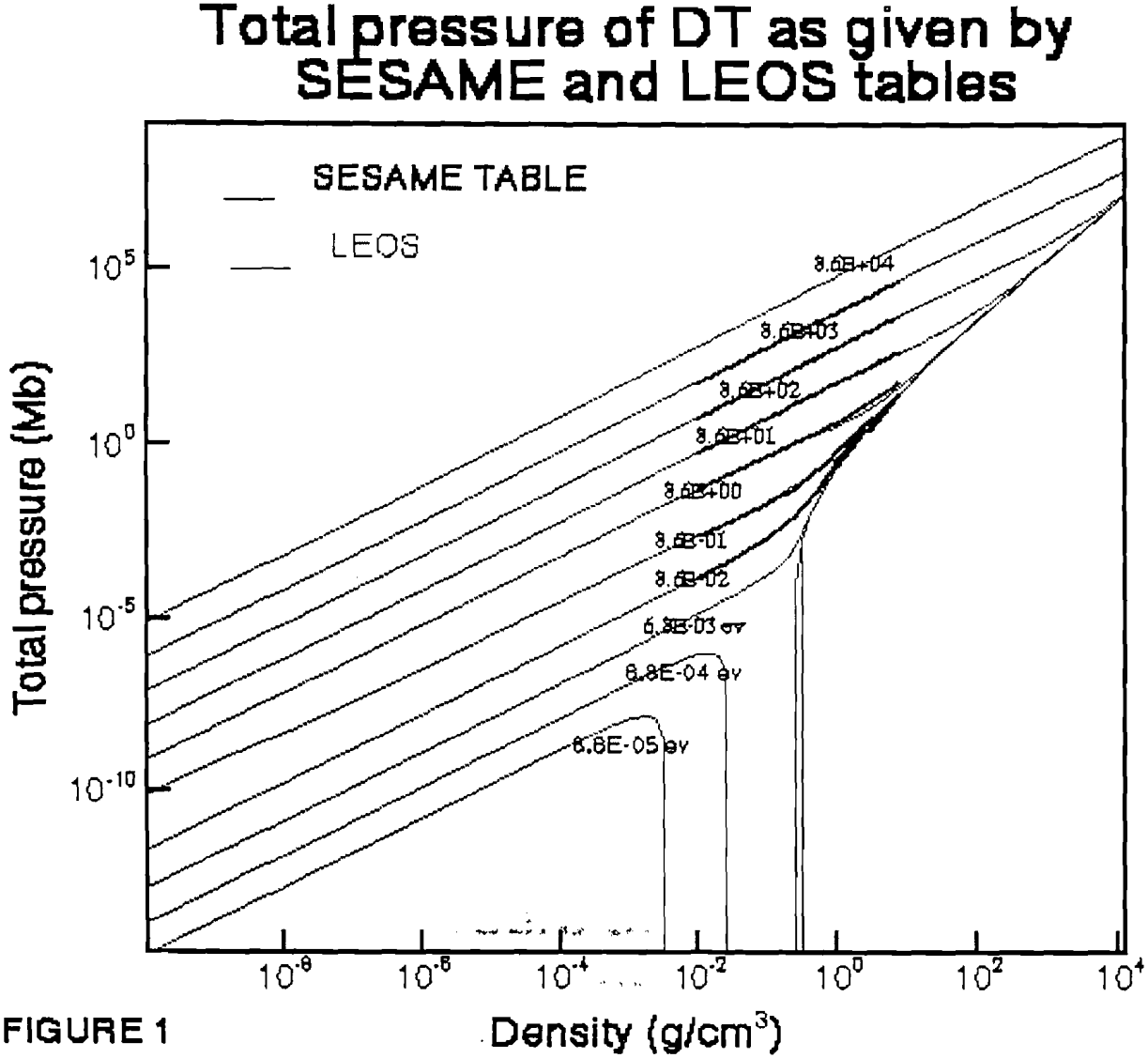
Total pressure of DT as given by SESAME and LEOS tables
SESAME TABLE
LEOS
8.6E+04
8.6E+03
8.6E+02
8.6E+01
8.6E+00
8.6E-01
8.6E-02
6.8E-03 ev
6.8E-04 ev
6.8E-05 ev
Total pressure (Mb)
10^{5}
10^{0}
10^{-5}
10^{-10}
10^{-8}
10^{-6}
10^{-4}
10^{-2}
10^{0}
10^{2}
10^{4}
Density (g/cm^3)

FIGURE 1

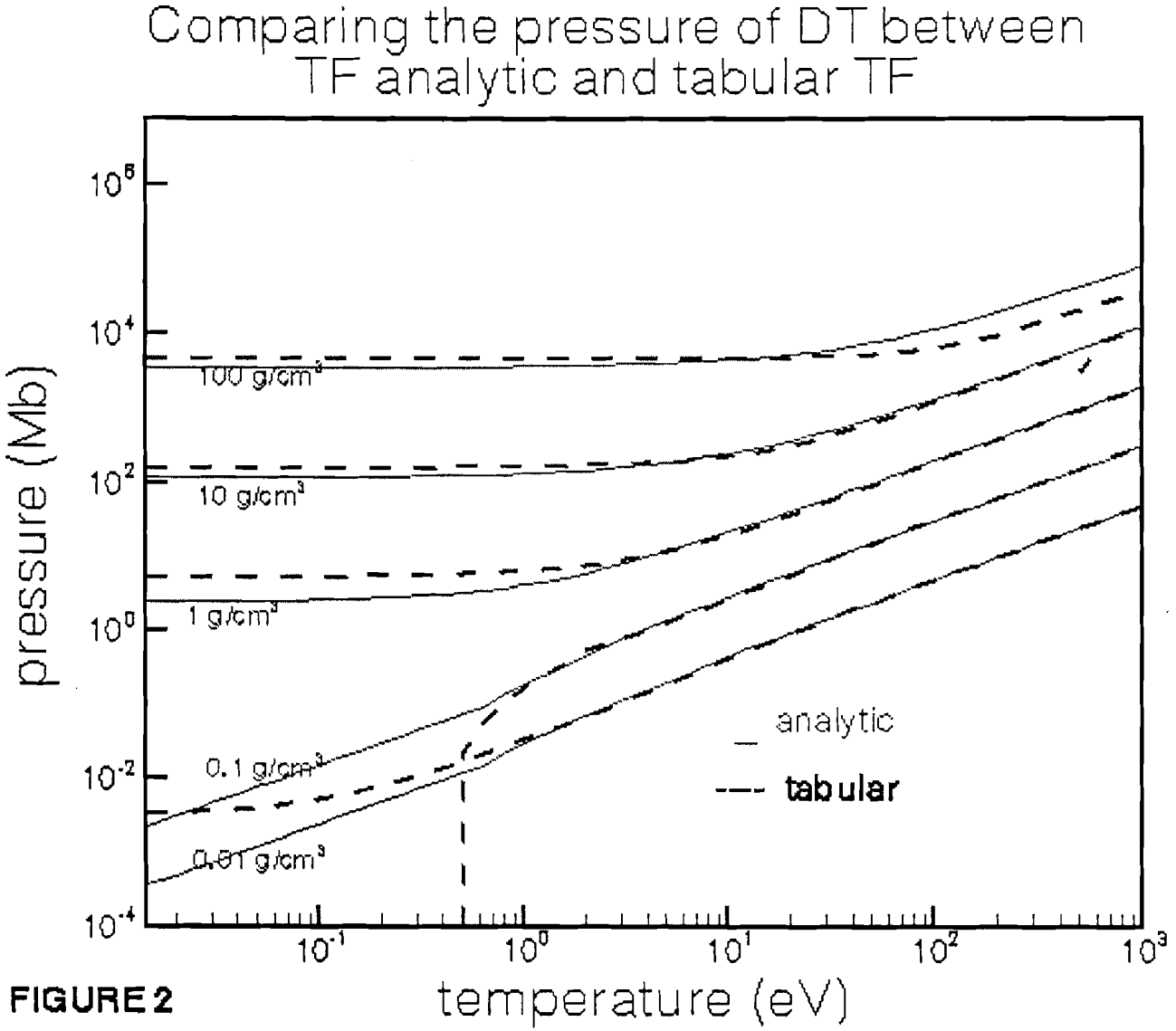
Comparing the pressure of DT between
TF analytic and tabular TF
pressure (Mb)
10^{6}
10^{4}
10^{2}
10^{0}
10^{-2}
10^{-4}
100 g/cm^3
10 g/cm^3
1 g/cm^3
0.1 g/cm^3
0.01 g/cm^3
analytic
tabular
10^{-1}
10^{0}
10^{1}
10^{2}
10^{3}
temperature (eV)

FIGURE 2

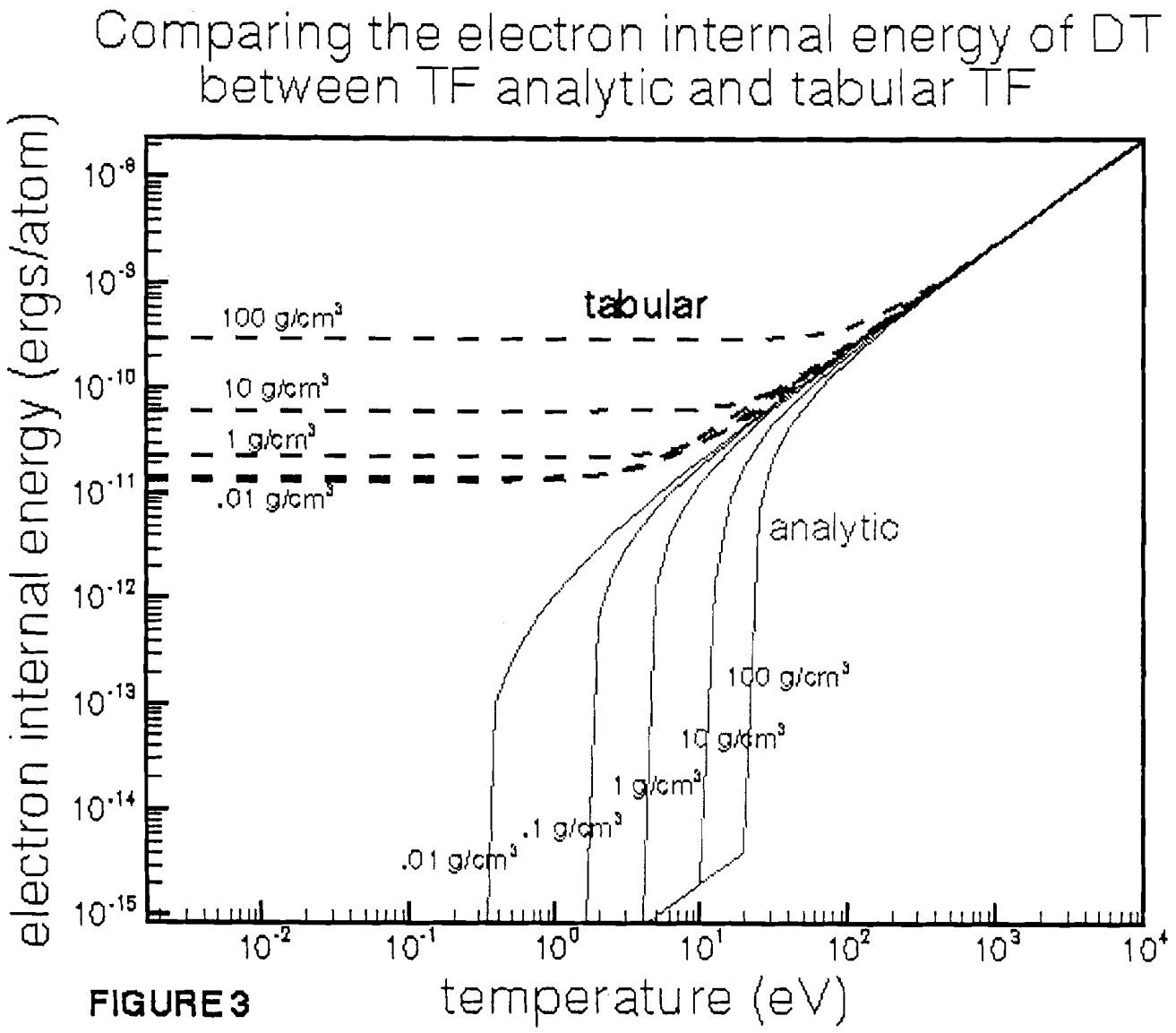
Comparing the electron internal energy of DT between TF analytic and tabular TF
electron internal energy (ergs/atom)
temperature (eV)
tabular
100 g/cm³
10 g/cm³
1 g/cm³
.01 g/cm³
analytic
100 g/cm³
10 g/cm³
1 g/cm³
.1 g/cm³
.01 g/cm³

FIGURE 3

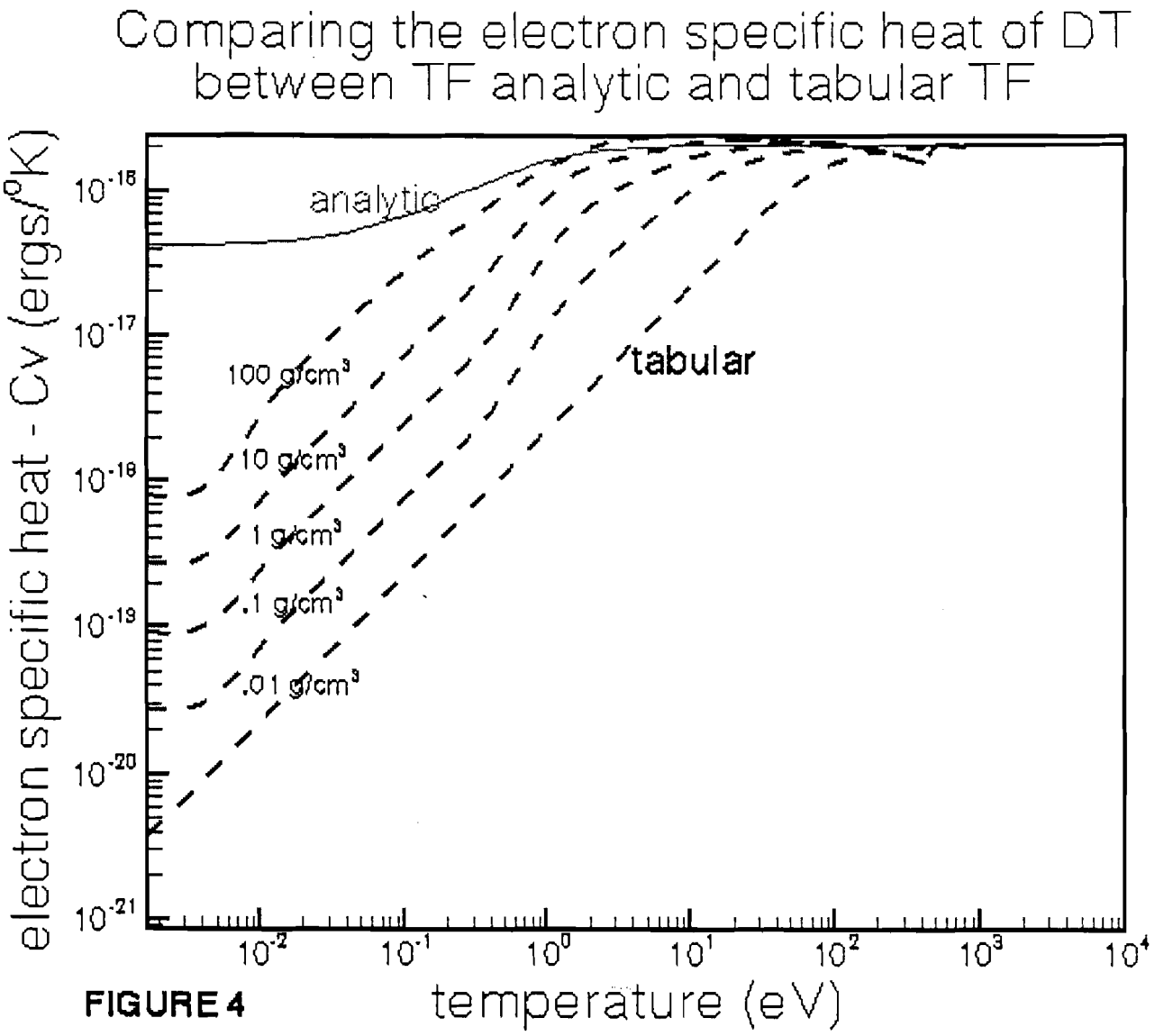
Comparing the electron specific heat of DT
between TF analytic and tabular TF
electron specific heat - Cv (ergs/°K)
temperature (eV)
analytic
tabular
100 g/cm³
10 g/cm³
1 g/cm³
.1 g/cm³
.01 g/cm³
10⁻¹⁶
10⁻¹⁷
10⁻¹⁸
10⁻¹⁹
10⁻²⁰
10⁻²¹
10⁻²
10⁻¹
10⁰
10¹
10²
10³
10⁴

FIGURE 4

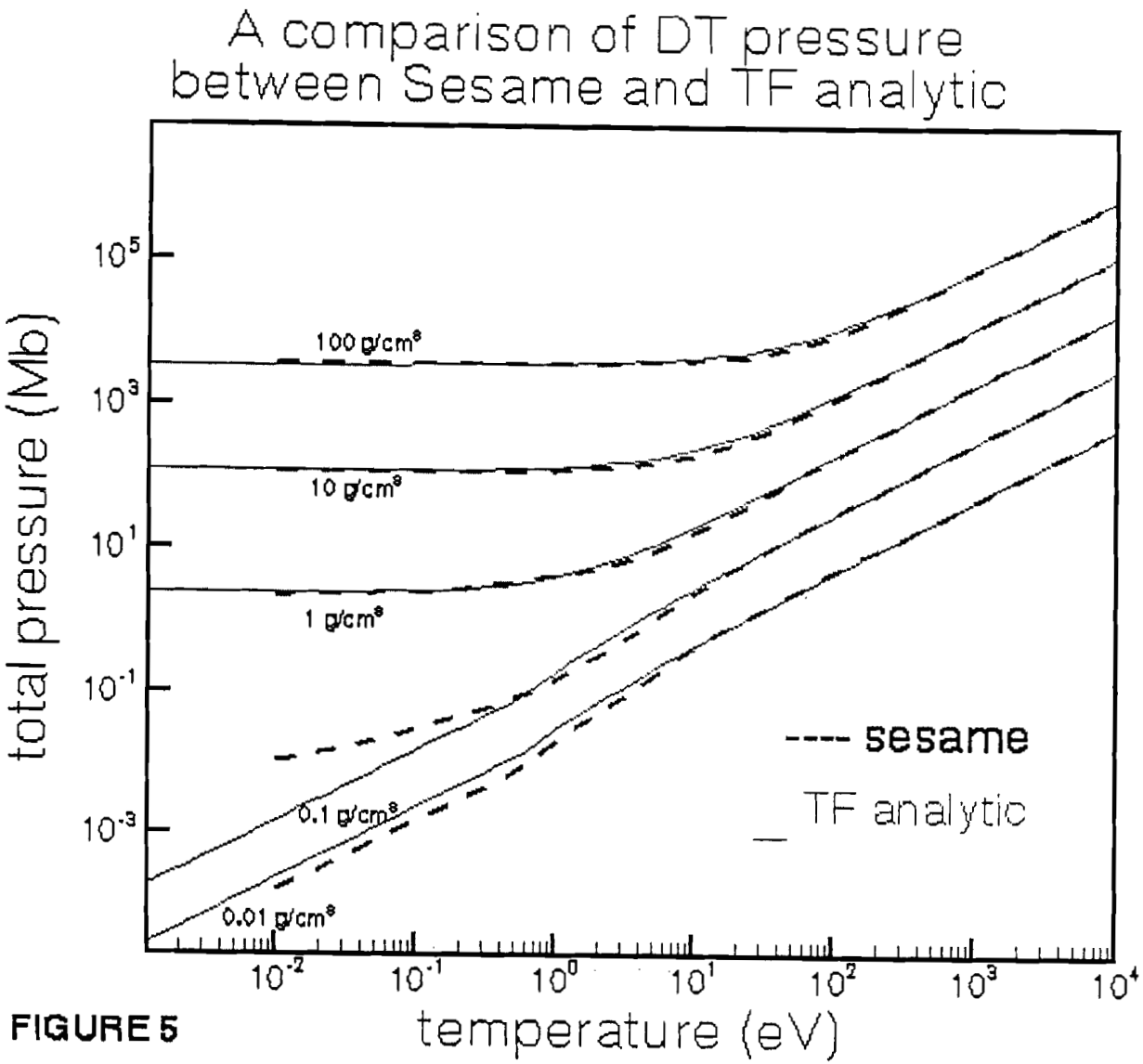
A comparison of DT pressure
between Sesame and TF analytic
total pressure (Mb)
temperature (eV)
100 g/cm³
10 g/cm³
1 g/cm³
0.1 g/cm³
0.01 g/cm³
---- sesame
_ TF analytic
10⁵
10³
10¹
10⁻¹
10⁻³
10⁻²
10⁻¹
10⁰
10¹
10²
10³
10⁴

FIGURE 5

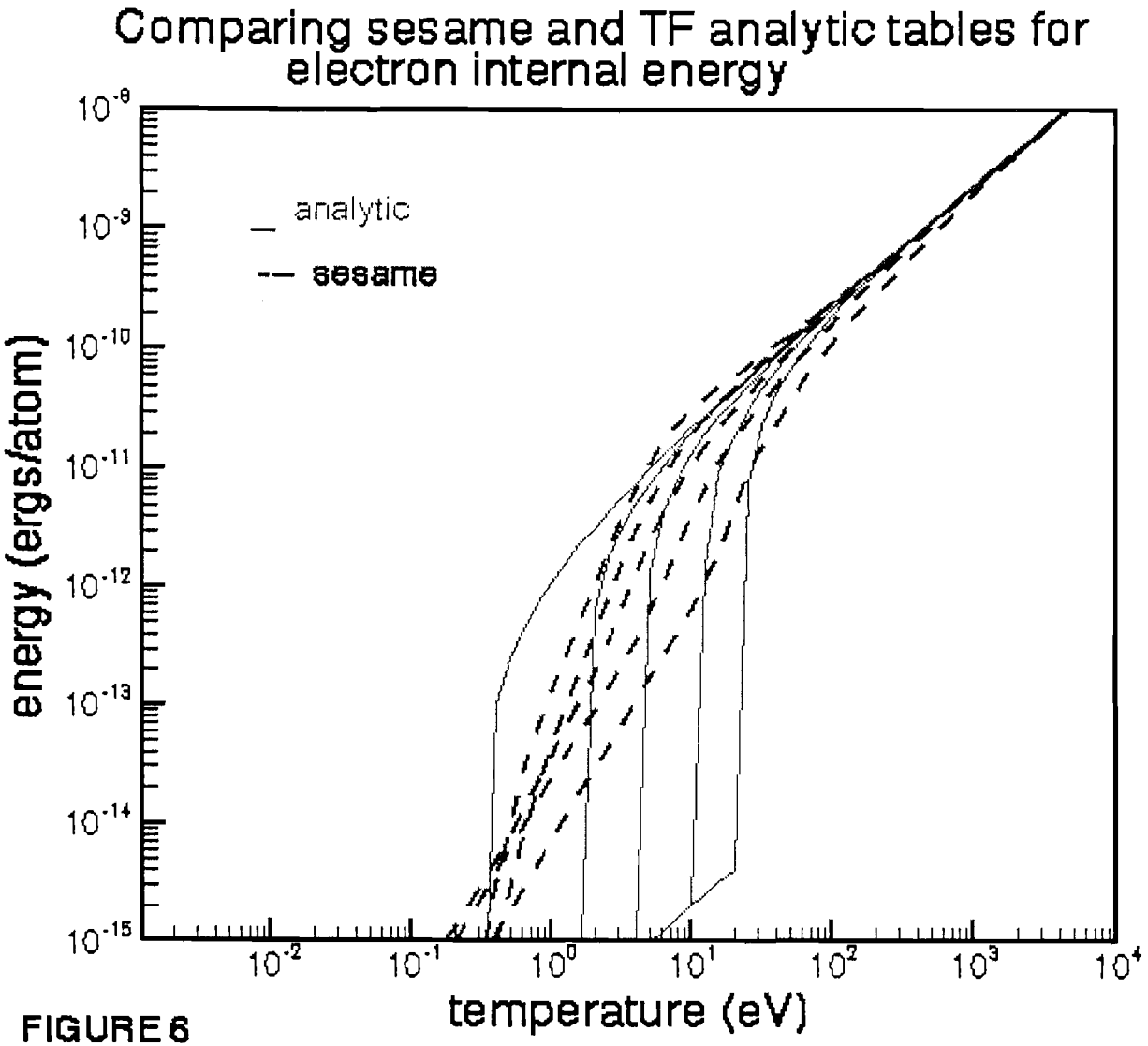
Comparing sesame and TF analytic tables for electron internal energy
analytic
sesame
energy (ergs/atom)
temperature (eV)
10^{-8}
10^{-9}
10^{-10}
10^{-11}
10^{-12}
10^{-13}
10^{-14}
10^{-15}
10^{-2}
10^{-1}
10^{0}
10^{1}
10^{2}
10^{3}
10^{4}

FIGURE 6

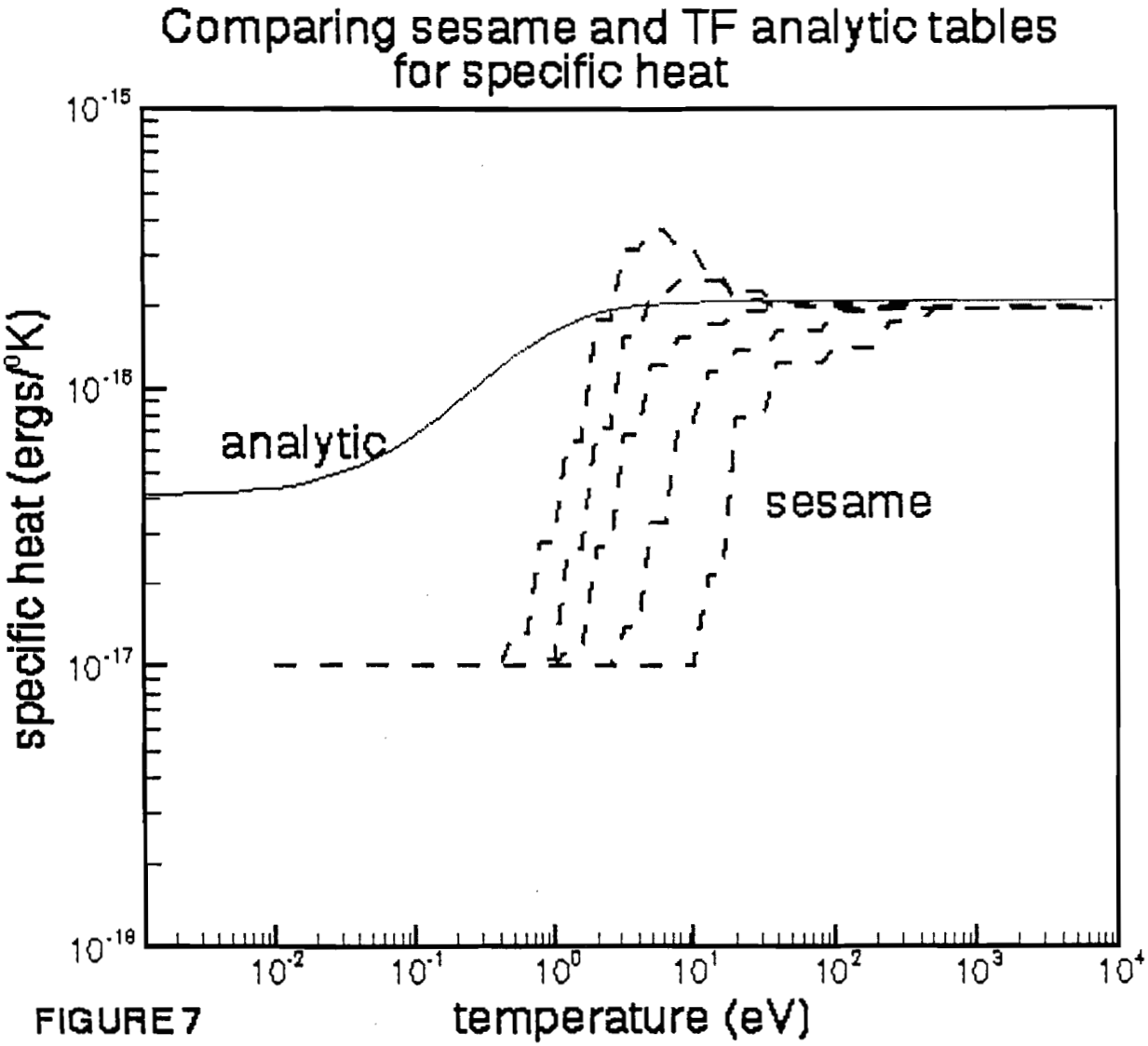
Comparing sesame and TF analytic tables
for specific heat
specific heat (ergs/°K)
10^-15
10^-16
10^-17
10^-18
analytic
sesame
10^-2
10^-1
10^0
10^1
10^2
10^3
10^4
temperature (eV)

FIGURE 7

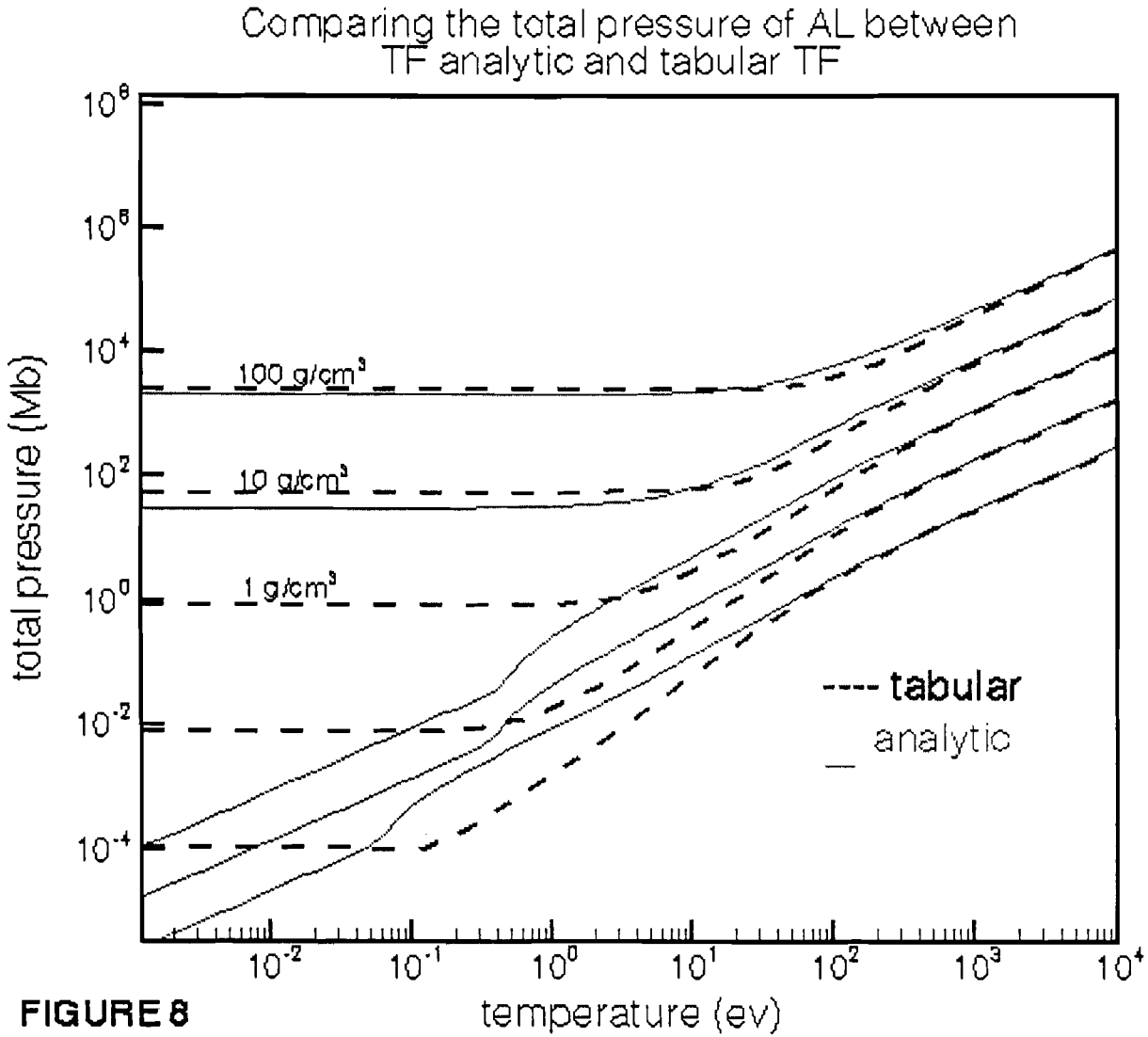
Comparing the total pressure of AL between
TF analytic and tabular TF
total pressure (Mb)
10^{6}
10^{6}
10^{4}
10^{2}
10^{0}
10^{-2}
10^{-4}
100 g/cm^3
10 g/cm^3
1 g/cm^3
---- tabular
_ analytic
10^{-2}
10^{-1}
10^{0}
10^{1}
10^{2}
10^{3}
10^{4}
temperature (ev)

FIGURE 8

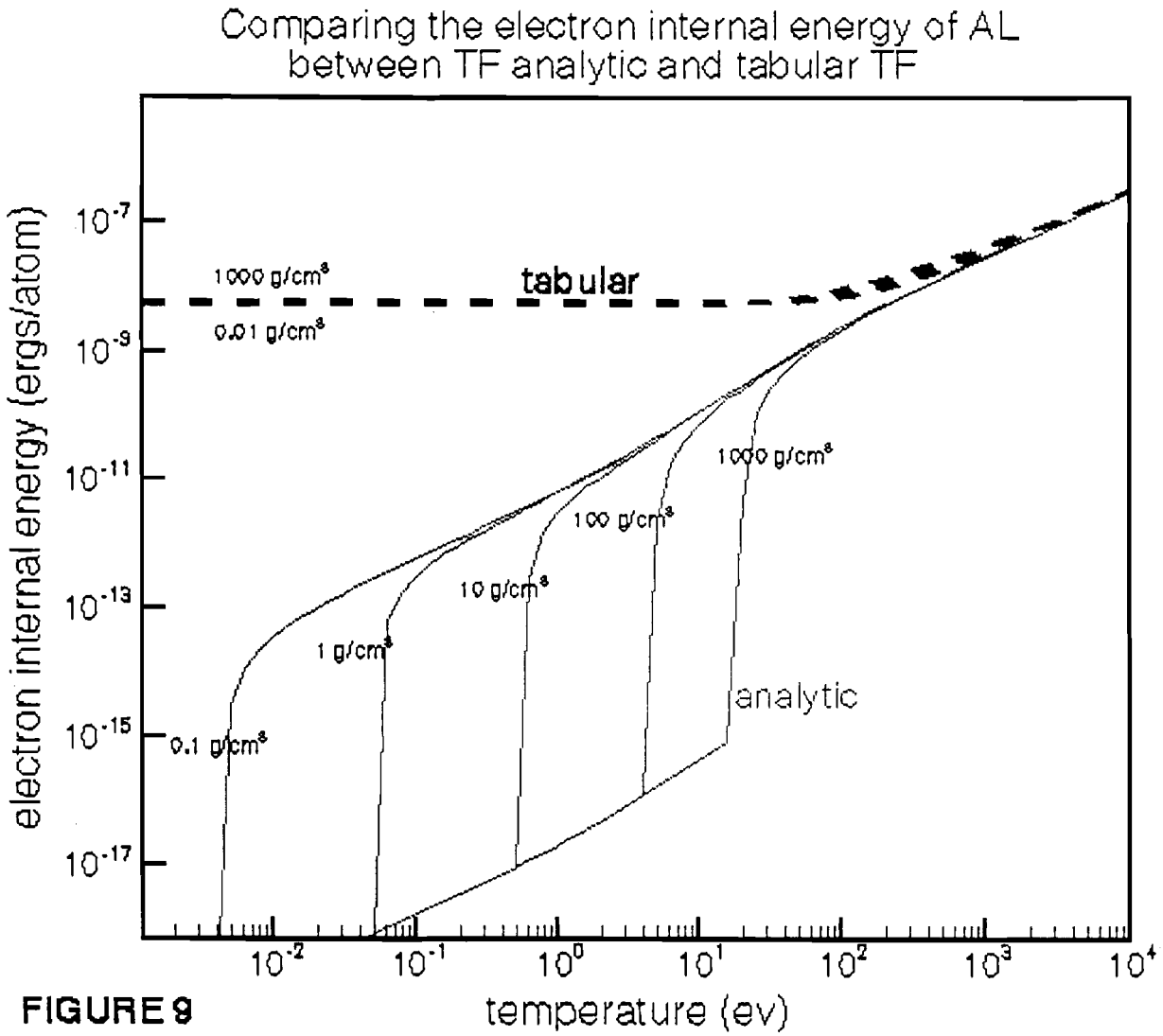
Comparing the electron internal energy of AL
between TF analytic and tabular TF
electron internal energy (ergs/atom)
temperature (ev)
tabular
1000 g/cm³
0.01 g/cm³
0.1 g/cm³
1 g/cm³
10 g/cm³
100 g/cm³
1000 g/cm³
analytic
10⁻⁷
10⁻⁹
10⁻¹¹
10⁻¹³
10⁻¹⁵
10⁻¹⁷
10⁻²
10⁻¹
10⁰
10¹
10²
10³
10⁴

FIGURE 9

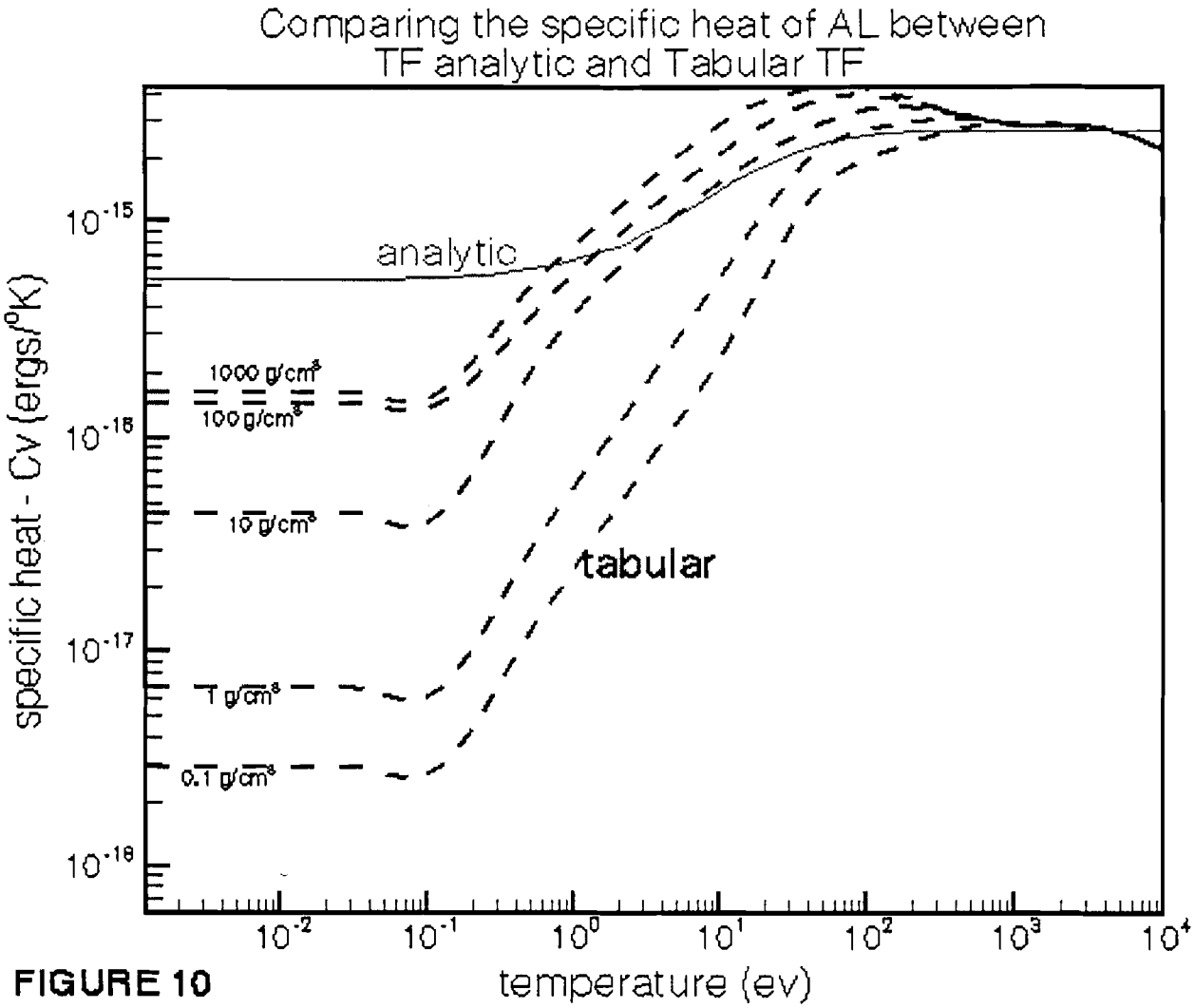
Comparing the specific heat of AL between
TF analytic and Tabular TF
analytic
tabular
1000 g/cm³
100 g/cm³
10 g/cm³
1 g/cm³
0.1 g/cm³
specific heat - Cv (ergs/°K)
temperature (ev)
10⁻¹⁵
10⁻¹⁶
10⁻¹⁷
10⁻¹⁸
10⁻²
10⁻¹
10⁰
10¹
10²
10³
10⁴

FIGURE 10

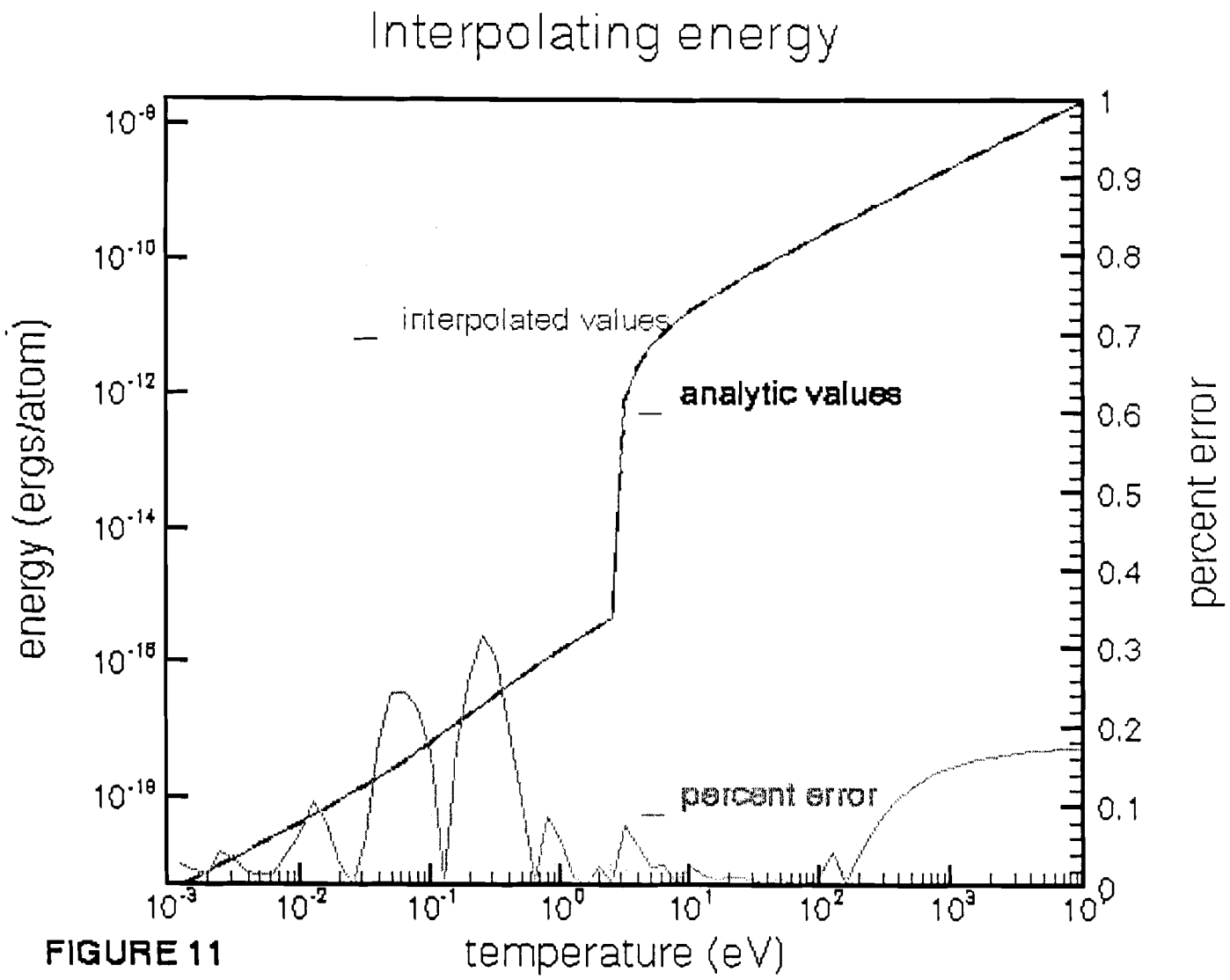
Interpolating energy
energy (ergs/atom)
temperature (eV)
percent error
interpolated values
analytic values
percent error
10^{-8}
10^{-10}
10^{-12}
10^{-14}
10^{-16}
10^{-18}
10^{-3}
10^{-2}
10^{-1}
10^{0}
10^{1}
10^{2}
10^{3}
10^{0}
1
0.9
0.8
0.7
0.6
0.5
0.4
0.3
0.2
0.1
0

FIGURE 11

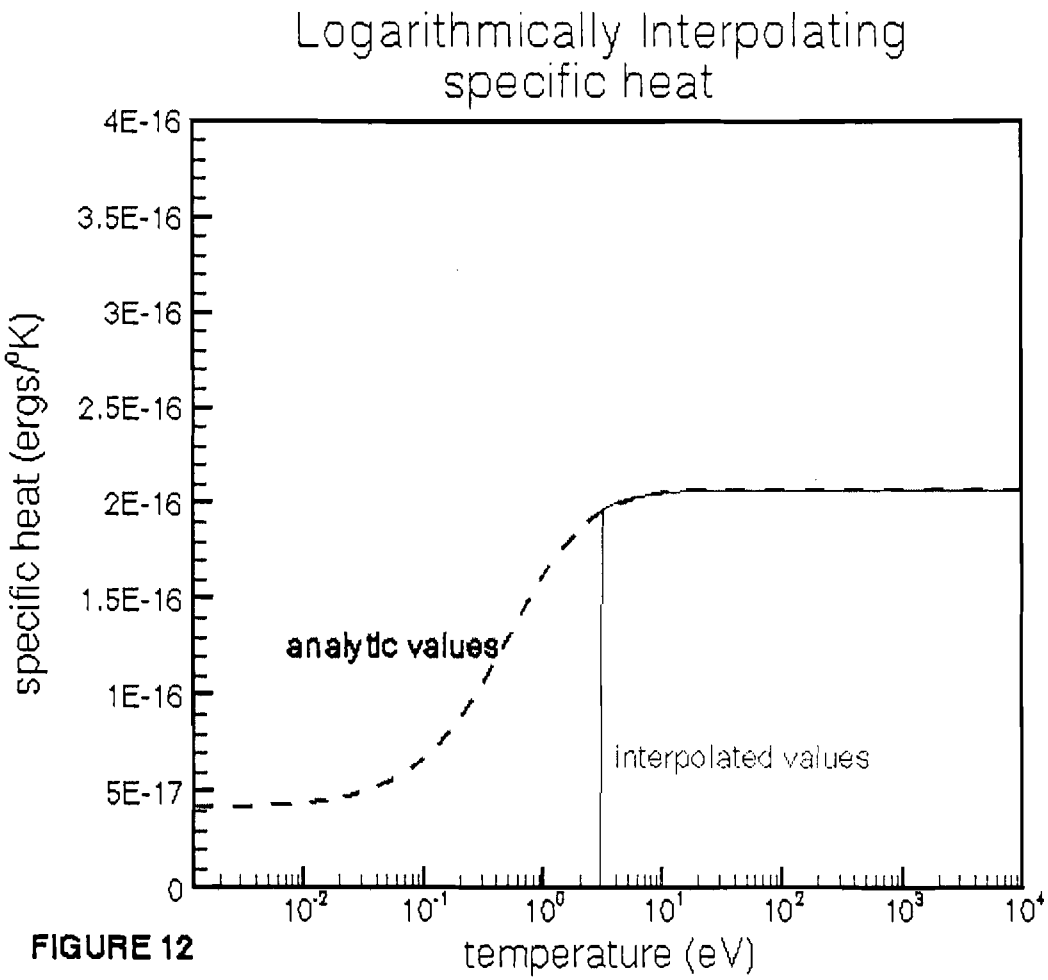
Logarithmically Interpolating
specific heat
4E-16
3.5E-16
3E-16
2.5E-16
2E-16
1.5E-16
1E-16
5E-17
0
specific heat (ergs/°K)
analytic values
interpolated values
10^{-2}
10^{-1}
10^{0}
10^{1}
10^{2}
10^{3}
10^{4}
temperature (eV)

FIGURE 12

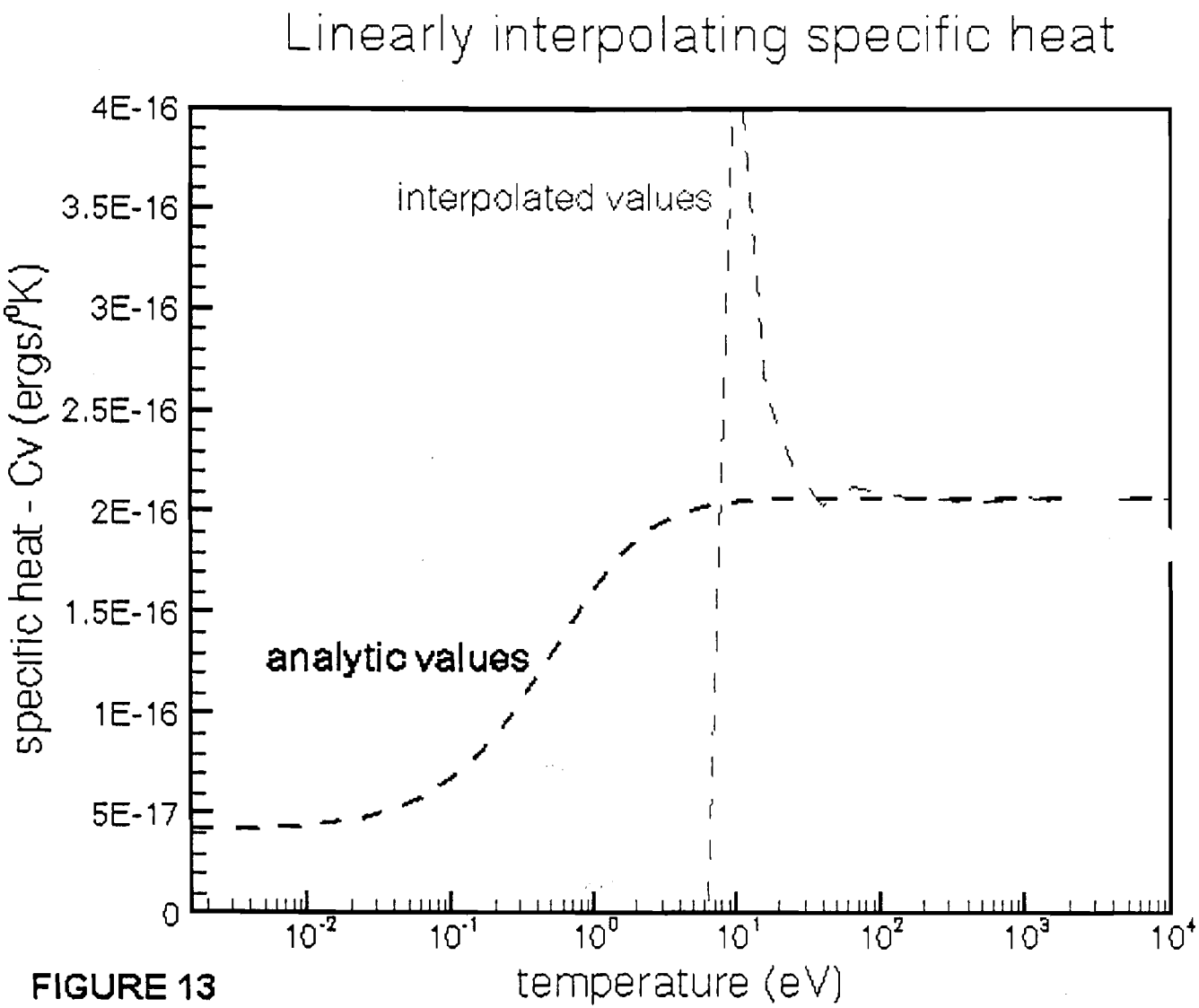
Linearly interpolating specific heat
4E-16
3.5E-16
3E-16
2.5E-16
2E-16
1.5E-16
1E-16
5E-17
0
specific heat - Cv (ergs/°K)
interpolated values
analytic values
10^-2
10^-1
10^0
10^1
10^2
10^3
10^4
temperature (eV)

FIGURE 13